



Annealing on the structure and properties evolution of the CoCrFeNiCuAl high-entropy alloy

K.B. Zhang^a, Z.Y. Fu^{a,*}, J.Y. Zhang^a, J. Shi^b, W.M. Wang^a, H. Wang^a, Y.C. Wang^a, Q.J. Zhang^a

^a State Key Laboratory of Advanced Technology for Materials Synthesis and Processing, Wuhan University of Technology, Wuhan 430070, China

^b College of Physics Science and Technology, Wuhan University, Wuhan 430072, China

ARTICLE INFO

Article history:

Received 12 October 2009

Received in revised form

15 November 2009

Accepted 16 November 2009

Available online 15 June 2010

Keywords:

Annealing

Microstructure

Mechanical properties

Magnetic properties

ABSTRACT

The equiatomic multiprincipal CoCrFeNiCuAl high-entropy alloy was prepared using a vacuum arc melt casting method. The as-cast alloy was subsequently annealed at 1000 °C for 2 h and the annealing effects on the structure and properties evolution were investigated. The as-cast alloy is composed of simple BCC and FCC solid solutions. The “2” FCC phase precipitates from the ordered BCC matrix and the FCC phases become dominated after the alloy was annealed. Both alloys show typical cast-dendrite morphology and similar elemental segregation. The as-annealed alloy exhibits high strength and excellent ductility of 1.63 GPa and 34%, respectively. Both alloys possess high saturated magnetization and undergo a ferromagnetic transition.

© 2009 Elsevier B.V. All rights reserved.

1. Introduction

Traditional strategy for developing alloys is to select one or two elements as principal components for primary properties with other minor elements incorporated for definite microstructure and properties [1]. Formation of many intermetallic compounds and other complex structures may be anticipated with multiple principal elements, resulting in brittle samples, difficulty in processing and complication in analysis [2,3]. Recently, this concept has been broken by high-entropy alloy developed by Yeh et al. [4], which is defined as alloys that contain at least five principal elements with each elemental concentration between 5 and 35 at.%. The high-entropy alloys usually form simple solid solution phases, nanoscaled structure and even amorphous in the as-cast state [5–8].

From the viewpoint of thermodynamics, the high entropy of mixing can significantly reduce the free energy, and thus decreases the tendency to order and makes alloys more stable with multiprincipal elements, especially at high temperature. For the industrial application of high-entropy alloy, it is worthwhile to investigate the effects of high temperature annealing on the stability of structure and properties. The multiprincipal CoCrFeNiCuAl high-entropy alloy is the most widely studied high-entropy alloy system in the past decade [9–10]. In this paper, the equiatomic CoCrFeNiCuAl

alloy was prepared by vacuum arc melt casting and the as-cast alloy was subsequently heated for 2 h at 1000 °C. The effects of annealing treatment on the structure and properties evolution were investigated.

2. Experimental details

Alloy ingots with nominal composition of equiatomic CoCrFeNiCuAl were prepared by vacuum arc melt casting in a Ti-gettered high-purity argon atmosphere with a water-cooled copper mould. Elemental metal sheets (purity >99%) were utilized as the raw materials. The ingots were remelted four times to improve the chemical homogeneity. The crystal structure of the samples was characterized by Rigaku Ultima III X-ray diffractometer (XRD). The microstructure of the alloys was observed using scanning electron microscope (SEM, Hitachi-S3400N) and transmission electron microscopy (TEM, JEOL JEM-2010). The chemical compositions of different regions were calculated from the results of energy-dispersive X-ray spectrometer (EDX) equipped with the SEM. Hardness measurements were conducted using a Visker hardness tester (Wolpert-430SVD) under a load of 49 N for 15 s. At least seven tests were conducted to obtain the average values. Room-temperature compressive properties of $\Phi 4$ mm \times 10 mm cylindrical samples were measured on MTS810 testing machine with a loading speed of 1 mm/min. The magnetic properties were conducted on the ADE Model 4 HF vibrating sample magnetometer (VSM).

3. Results and discussions

3.1. Crystal structure evolution

Fig. 1 shows the XRD patterns of the as-cast and as-annealed CoCrFeNiCuAl high-entropy alloys. Diffraction peaks corresponding to a simple ordered BCC and disordered FCC solid solutions are observed in the as-cast alloy. The ordered BCC phase exhibits as

* Corresponding author. Tel.: +86 27 87865484; fax: +86 27 87215421.

E-mail address: zyfu@whut.edu.cn (Z.Y. Fu).

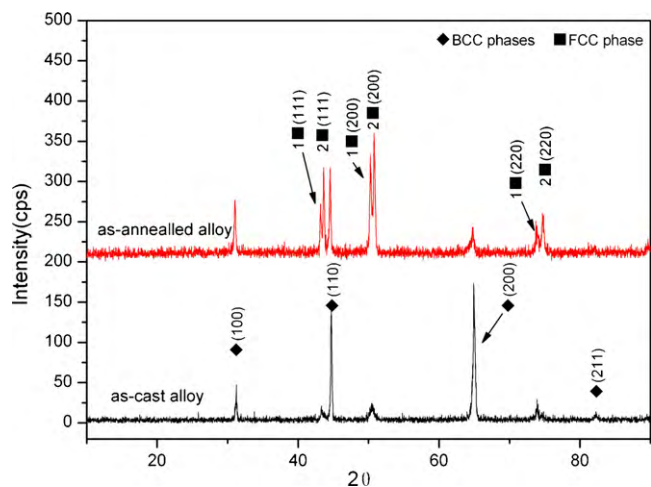


Fig. 1. XRD patterns of the as-cast and as-annealed CoCrFeNiCuAl high-entropy alloys.

the matrix while the FCC phases show as the minor ones. The “2” FCC phase precipitates beside the ordered BCC matrix and becomes dominated after the alloy was annealed at 1000 °C for 2 h, which can hardly be distinguished from the “1” FCC phase in the as-cast alloy. The lattice constants of the two FCC phases (“1” and “2” FCC) are estimated to be 0.3624 and 0.3591 nm by linearity extrapolation method, while the ordered BCC phase shows a lattice constant of 0.2875 nm. From the mixing enthalpy of the binary metallic system, the CoCrFeNiCuAl alloy can hardly form simple solid solution under equilibrium conditions. The BCC and FCC phases in the as-cast CoCrFeNiCuAl high-entropy alloy can be designated as supersaturated solid solutions prepared by arc melt casting equipped with rapid cooling solidification [11]. As the metallic elements exhibit various atomic radiuses, the random substitution among them will definitely increase the lattice distortion energy, which leads to the formation of metastable phases under nonequilibrium state. Stable solid solutions would precipitate to release the lattice distortion energy when the supersaturated solid solution alloy is annealed at high temperature.

The XRD result reveals a remarkable influence of annealing on the crystal structure evolution of the CoCrFeNiCuAl high-entropy alloy. Although with obvious three phases, the as-annealed CoCrFeNiCuAl alloy shows simple solid solution structure and the phase number is well below the maximum equilibrium number allowed by the Gibbs phase rule. The formation of simple solid solution is attributed to the high mixing entropy with multiple principal elements [4]. According to Gibbs free energy described as follows:

$$G_{\text{mix}} = H_{\text{mix}} - TS_{\text{mix}}$$

The high entropy of mixing can significantly lower the free energy, thus lowering the tendency to order and consequently making random solid solution more stable than intermetallics and other complex phases.

3.2. Microstructure and chemical composition analysis

Fig. 2 presents the microstructure images of the as-cast CoCrFeNiCuAl high-entropy alloy. Cast-dendrite morphology of dendrite matrix and bone-shaped interdendrite phase are observed in the low magnified image (Fig. 2(a)). According to the XRD analysis, the dendrite is confirmed of the ordered BCC phase while the interdendrite can be designated as the FCC structure. The high magnified image shown in Fig. 2(b) reveals the nanoscaled basket-weaved structure of the dendrite matrix. This netlike structure can

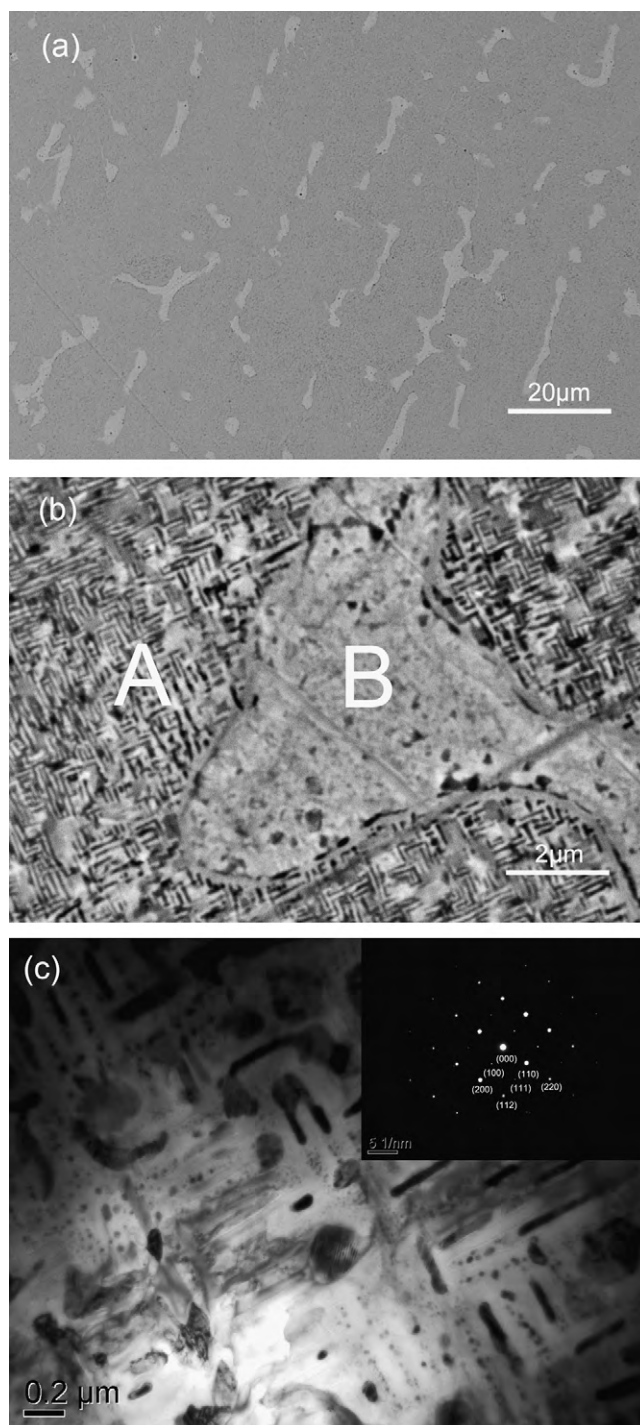


Fig. 2. Microstructure of the as-cast CoCrFeNiCuAl high-entropy alloy: (a) low magnified SEM image, (b) high magnified SEM image and (c) TEM bright field image and SAED pattern.

be regarded as modulated plates resulting from spinodal decomposition which has been reported by Soffa and Laughlin [12]. The corresponding select area electron diffraction (SAED) pattern of the dendrite matrix is shown in Fig. 2(c). The SAED pattern shows an ordered BCC superlattice structure, which is in agreement with the XRD result and can further confirm the ordered BCC structure of the dendrite matrix. Nanoscaled modulated plate with 70 nm in width is observed in the TEM bright field image in Fig. 2(c). The modulated plates are mainly in two directions perpendicular with each other, which reflects the basket-weaved structure

Table 1
Chemical compositions of the as-cast and as-annealed CoCrFeNiCuAl high-entropy alloys.

Alloy	Zone	Co	Cr	Fe	Ni	Cu	Al
As-cast	A	18.5	20.88	17.66	16.74	8.61	17.61
	B	6.17	3.18	4.75	10.92	61.39	13.58
As-annealed	A	17.84	12.95	15.74	19.85	09.43	24.01
	B	16.81	21.89	17.71	17.73	06.74	19.56
	C	7.61	5.96	6.86	10.41	57.73	11.45

Table 2
Mechanical properties of the as-cast and as-annealed CoCrFeNiCuAl high-entropy alloys.

Alloy	σ_{\max} (GPa)	ε_p (%)	Visker hardness
As-cast	1.82	20.7	515.5
As-annealed	1.63	34	369.8

in the dendrite matrix. Nanoscaled ellipsoidal particles (less than 100 nm) were also observed among the modulated plate structure. The nanocrystalline structure is rarely seen in the corresponding states of conventional alloys or bulk amorphous alloys. From the viewpoint of kinetics, long-range diffusion for phase separation is sluggish in solid high-entropy alloys with multiprincipal elements. Difficulty in substitutional diffusion of elements in these alloys and interactions among interdiffusion during partitioning lowered the rates of nucleation and growth, leading to the formation of nanostructured crystallites [8].

The chemical compositions of the dendrite and interdendrite regions (labelled as “A” and “B” in Fig. 2(b)) calculated from the EDX results are listed in Table 1. The dendrite phase is obviously rich in Co, Cr, Fe while the interdendrite region shows Cu enrichment. The elemental segregation can be explained by the mixing enthalpies among the principal metallic elements [13]. As Cu shows relatively higher positive enthalpies with Co, Cr and Fe, it is repelled from the dendrite region by these elements. Accordingly, Ni and Al exhibit lower positive enthalpies with Cu and thus they are partly attracted to the interdendrite region [14].

The as-annealed CoCrFeNiCuAl high-entropy alloy exhibits similar cast-dendrite morphology with the as-cast alloy (shown in Fig. 3(a)). However, the nanoscaled structure of modulated plate disappears (Fig. 3 (b)). It can be confirmed from the analysis of XRD and SEM that the black and grey phase (marked as “A” and “B” in Fig. 3(b)) can be designated as the ordered BCC and the “2” FCC phases while the white phase (“C” in Fig. 3(b)) must be the “1” FCC phase. The “2” FCC phase is precipitated from the ordered BCC matrix after annealing, which can hardly be observed in the as-cast alloy. Fig. 3(c) shows the TEM bright field image of the as-annealed alloy and the corresponding SAED pattern of the precipitation. The SAED pattern shows a disordered FCC structure in accordance with the XRD result. The precipitation with a particle size of 1 μm is observed in the TEM bright field image. The structural coarsening results from crystal growth induced by the high temperature heat treatment. The EDX result (shown in Table 1) reveals that the as-annealed CoCrFeNiCuAl alloy exhibits similar elemental segregation as the as-cast alloy. The “2” FCC phase is rich in Fe and Cr, which can be explained by the difference of chemical mixing enthalpy as well.

3.3. Mechanical properties

Fig. 4 depicts the room-temperature compressive true stress–strain curves of the as-cast and as-annealed CoCrFeNiCuAl high-entropy alloys. The detailed data of the mechanical properties are listed in Table 2. The as-cast and as-annealed alloys exhibit high hardness of 515.5 and 369.8 HV, respectively. The compressive

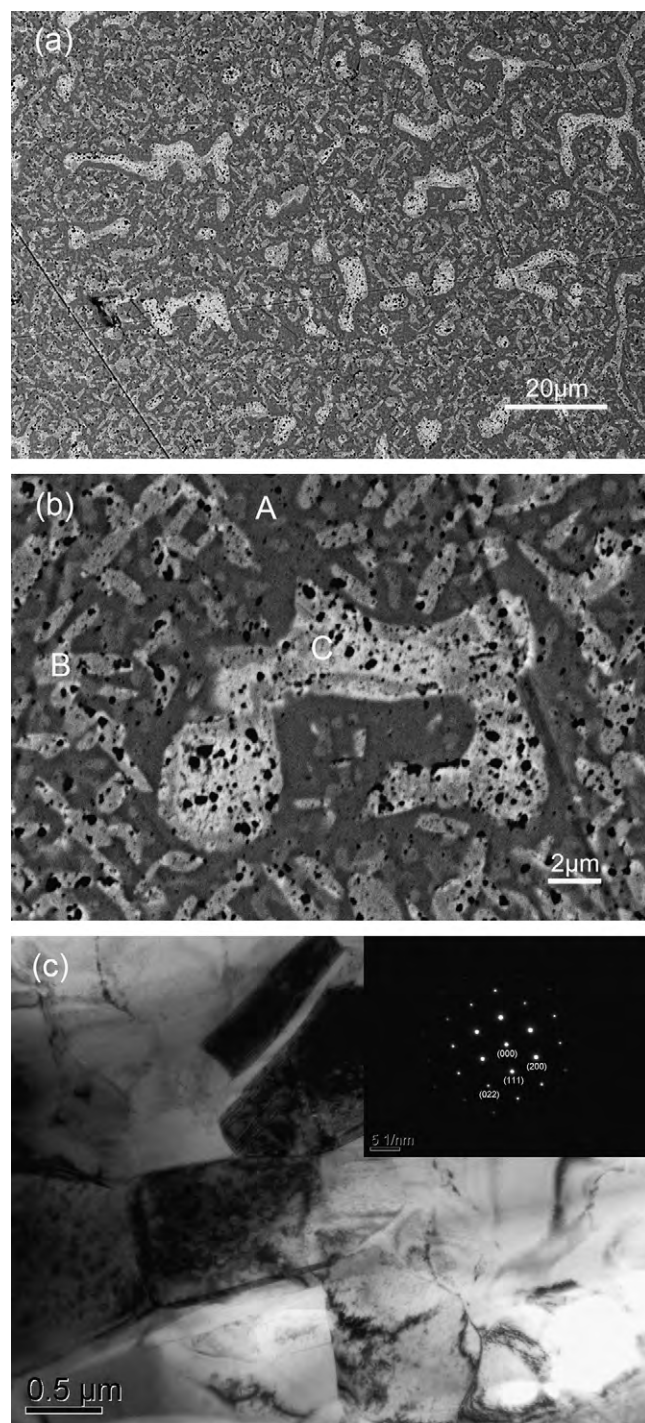


Fig. 3. Microstructure of the as-annealed CoCrFeNiCuAl high-entropy alloy: (a) low magnified SEM image, (b) high magnified SEM image and (c) TEM bright field image and SAED pattern.

strength and plastic strain of the as-cast CoCrFeNiCuAl alloy reach 1.82 GPa and 20.7%. A saw-toothed work hardening curve is observed when the as-cast alloy is yielding at high pressure. The compressive strength of the as-annealed alloy decreases slightly to 1.63 GPa. However, it exhibits extremely high plastic strain of 34% and large saw-toothed work hardening capability. In the work hardening curve of the as-annealed alloy, the yielding strength fluctuates and the next yielding takes place at a higher pressure, which facilitates the alloy with higher strength and ductility. Another yielding platform turns up at a lower strength when the

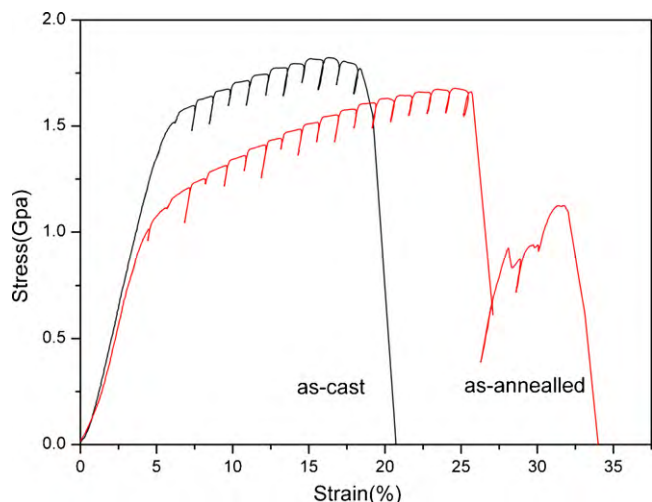


Fig. 4. Compressive true stress-strain curves of the as-cast and as-annealed CoCrFeNiCuAl high-entropy alloys.

alloy was broken down from high pressure. This kind of yielding platform is rarely seen in traditional alloys, which can further increase the ductility of sample and prevent it from collapsing at sudden.

The simultaneous appearance of high strength and ductility is hardly seen in traditional metals and alloys, especially for alloys after high temperature annealing. The high strength of the as-cast CoCrFeNiCuAl high-entropy alloy can be attributed to the solid solution strength and strong bonding effect among the alloy metallic elements [15]. On the other hand, the nanosized modulated plate matrix can also enhance the strength of the as-cast alloy. The excellent ductility and large work hardening capacity can be explained by the phase composition of the as-annealed CoCrFeNiCuAl alloy. According to the basic structural factor, the structure with more slip system leads to lower lattice friction during dislocation motion and thus increases the ductility of samples [16]. The FCC structure possesses 48 slip system more than that of the BCC structure with 12 slip system. As the “2” FCC phase precipitates from the matrix BCC phase in the as-annealed alloy, the FCC phases become dominant and accordingly the ductility and work hardening effect increase.

3.4. Magnetic properties

Fig. 5(a) presents the magnetic hysteresis loops of the as-cast and as-annealed CoCrFeNiCuAl high-entropy alloys measured at room temperature. Both alloys show excellent soft magnetic properties. Saturated magnetizations (M_s), remanence ratio (M_r/M_s) and coercivity (H_c) of the as-cast and as-annealed alloys are estimated to be 38.18 emu/g, 5.98%, 45 Oe and 16.08 emu/g, 3.01%, 15 Oe, respectively. Zhang and co-workers [17] had investigated the magnetic properties of CoCrCuFeNiTi_x alloys and they exhibited saturated magnetization lower than 2 emu/g. Compared with the magnetic properties of bulk metals, both the as-cast and as-annealed CoCrFeNiCuAl alloys show high M_s and low H_c . The alloys show comparable magnetic properties with the soft ferrite and can be utilized as soft magnetic materials [18]. On the other hand, the as-cast alloy exhibits a similar superparamagnetic curve, which can be attributed to the nanoscaled microstructure [19]. The decrement of M_s in the as-annealed alloy is resulted from the structure coarsening and phase transformation. Fig. 5(b) depicts the temperature dependence of magnetization ($M(T)$) curves of the as-cast and as-annealed alloys while cooling the alloys at 200 Oe. The results clearly reveal a ferromagnetic transition of both alloys. The as-cast alloy shows higher magnetization than the as-annealed

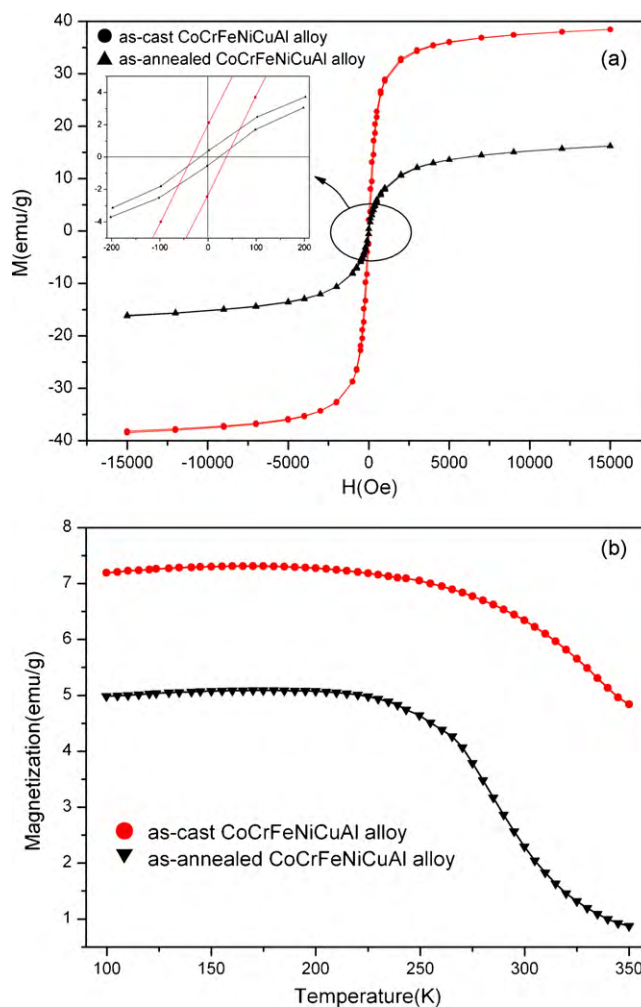


Fig. 5. Magnetization curves of the as-cast and as-annealed CoCrFeNiCuAl high-entropy alloys: (a) the hysteresis loops and (b) the temperature dependence of magnetization ($M(T)$) curves while cooling the alloys at 200 Oe.

alloy at all temperatures. The other point of the $M(T)$ curves is the high T_c of both alloys.

4. Conclusions

The as-cast CoCrFeNiCuAl high-entropy alloy exhibits simple BCC and FCC solid solution structure. Cast-dendrite morphology with nanoscaled modulated plate dendrite and bone-shaped interdendrite phase is observed. The “2” FCC phase precipitates from the ordered BCC matrix and the FCC phases become dominated when the alloy was annealed 2 h at 1000 °C. The interdendrite regions are rich in Cu while the dendrite regions exhibit Co, Cr, Fe enrichment in both the as-cast and as-annealed alloys. The as-cast alloy shows high strength and good plasticity of 1.82 GPa and 20.7%, respectively. The as-annealed alloy exhibits excellent ductility of 34% and high work hardening capability as well as a yielding platform at a lower strength. The as-cast and as-annealed CoCrFeNiCuAl high-entropy alloys exhibit high M_s of 38.178 emu/g and 16.082, and they both undergo a ferromagnetic transition.

Acknowledgements

The authors would like to acknowledge the financial support by the National Natural Science Foundation of China (NNSFC) under

grant nos. 50772081 and 50821140308, and the Ministry of Education of China under grant no. PCSIRT0644.

References

- [1] A. Inoue, *Acta Mater.* 48 (2000) 1383–1395.
- [2] A.L. Greer, *Nature* 366 (1996) 150.
- [3] H. Baker, *Metals Handbook*, 3, 10th ed., ASM International, Metal Park, OH, 1992.
- [4] J.W. Yeh, S.K. Chen, S.J. Lin, J.Y. Gan, T.S. Chin, T.T. Shun, C.H. Tsau, S.Y. Chang, *Adv. Eng. Mater.* 6 (2004) 299–303.
- [5] B. Cantor, I.T.H. Chang, P. Knight, A.J.B. Vincent, *Mater. Sci. Eng. A* 375 (2004) 213–218.
- [6] Y.J. Zhou, Y. Zhang, Y.L. Wang, G.L. Chen, *Appl. Phys. Lett.* 90 (2007) 181904.
- [7] Y.P. Wang, B.S. Li, M.X. Ren, C. Yang, H.Z. Fu, *Mater. Sci. Eng. A* 491 (2008) 154–158.
- [8] K.B. Zhang, Z.Y. Fu, J.Y. Zhang, W.M. Wang, H. Wang, Y.C. Wang, Q.J. Zhang, J. Shi, *Mater. Sci. Eng. A* 508 (2009) 214–219.
- [9] C.C. Tung, J.W. Yeh, T.T. Shun, S.K. Chen, Y.S. Huang, H.C. Cheng, *Mater. Lett.* 61 (2007) 1–5.
- [10] C.J. Tong, Y.L. Chen, S.K. Chen, J.W. Yeh, T.T. Shun, C.H. Tsau, S.J. Lin, S.Y. Chang, *Metall. Mater. Trans. A36A* (2005) 881–893.
- [11] H. Jones, *Rapid Solidification of Metals and Alloys*, Monograph No. 8, The Institute of Metallurgist, London, England, 1982.
- [12] W.A. Soffa, D.E. Laughlin, *Proc. Int. on Solid–Solid Phase Transformation*, Pittsburgh, PA, August 10–14, ASM, Metals Park, OH, 1981, pp. 159–182.
- [13] U.S. Hsu, U.D. Huang, J.W. Yeh, S.K. Chen, Y.S. Huang, C.C. Yang, *Mater. Sci. Eng. A* 460 (2007) 403–408.
- [14] H. Zhang, B.W. Zhang, L.J. Wu, Z.Q. Wan, *Acta Phys. Sin.* 43 (1994) 1638–1647.
- [15] J.J. Harwood, *Proceedings of the ASM Seminar: Strengthening Mechanisms in Solids*, Metals Park, OH, 1960, p. 23.
- [16] G.E. Dieter, *Mechanical Metallurgy*, SI Metric Editions, McGraw–Hill Books Company, New York, 1988, p. 117.
- [17] X.F. Wang, Y. Zhang, Y. Qiao, G.L. Chen, *Intermetallics* 15 (2007) 357–362.
- [18] C. Miclea, C. Tanasoiu, C.F. Miclea, *J. Magn. Magn. Mater.* 290 (2005) 1506–1509.
- [19] S.R. Shinde, S.B. Ogale, J.S. Higgins, *Phys. Rev. Lett.* 92 (2004) 166601.